J|A|C|S
ARTICLES
Published on Web 10/04/2006

Cluster−Support Interactions and Morphology of MoS_2 Nanoclusters in a Graphite-Supported Hydrotreating Model Catalyst

Jakob Kibsgaard,[†] Jeppe V. Lauritsen,*[,†] Erik Lægsgaard,[†] Bjerne S. Clausen,[‡] Henrik Topsøe,[‡] and Flemming Besenbacher*[,†]

Contribution from the Interdisciplinary Nanoscience Center (iNANO) and Department of Physics and Astronomy, University of Aarhus, DK-8000 Aarhus C, Denmark, and Haldor Topsøe A/S, Nymøllevej 55, DK-2800 Lyngby, Denmark

Received July 18, 2006; E-mail: jvang@phys.au.dk; fbe@inano.au.dk

Abstract: Supported MoS_2 nanoparticles constitute the active component of the important hydrotreating catalysts used for industrial upgrading and purification of the oil feedstock for the production of fossil fuels with a low environmental load. We have synthesized and studied a model system of the hydrotreating catalyst consisting of MoS_2 nanoclusters supported on a graphite surface in order to resolve a number of very fundamental questions related to the atomic-scale structure and morphology of the active clusters and in particular the effect of a substrate used in some types of hydrotreating catalysts. Scanning tunneling microscopy (STM) is used to image the atomic-scale structure of graphite-supported MoS_2 nanoclusters in real space. It is found that the pristine graphite (0001) surface does not support a high dispersion of MoS_2, but by introducing a small density of defects in the surface, highly dispersed MoS_2 nanoclusters could be synthesized on the graphite. From high-resolution STM images it is found that MoS_2 nanoclusters synthesized at low temperature in a sulfiding atmosphere preferentially grow as single-layer clusters, whereas clusters synthesized at 1200 K grow as multilayer slabs oriented with the MoS_2(0001) basal plane parallel to the graphite surface. The morphology of both single-layer and multilayer MoS_2 nanoclusters is found to be preferentially hexagonal, and atom-resolved images of the top facet of the clusters provide new atomic-scale information on the MoS_2−HOPG bonding. The structure of the two types of catalytically interesting edges terminating the hexagonal MoS_2 nanoclusters is also resolved in atomic detail in STM images, and from these images it is possible to reveal the atomic structure of both edges and the location and coverage of sulfur and hydrogen adsorbates.

1. Introduction

The study of supported MoS_2 nanoclusters is of particular interest, since it has been established that the activity of the industrial-type hydrotreating catalyst used for upgrading and cleaning up oil feedstocks is related to MoS_2 nanoclusters as the active component, typically promoted with Ni or Co atoms.[1−3] Currently, an intense interest in improving such metal sulfide-based hydrotreating catalysts is driven by new legislation regarding fuel specifications, especially with respect to the level of sulfur-containing hydrocarbons in fuels.[4−6] However, due to the high structural complexity of the MoS_2-based catalyst, it has been difficult to extract detailed atomic-scale information on the real catalyst structure from traditional averaging characterization techniques,[1,7−10] and consequently basic insight into the morphology and atomic-scale structure of the active MoS_2-like nanoclusters has been lacking. In recent studies, it was possible for the first time to directly address the important questions related to the morphology and atomic-scale structures of both unpromoted and cobalt-promoted MoS_2 nanoclusters by imaging them with highly resolved scanning tunneling microscopy (STM).[11−13] In these studies, single-layer MoS_2 nanoclusters were grown on a gold single-crystal substrate to synthesize a well-characterized model system for the hydrotreating catalyst, which had a minimum of support interactions, as the gold is rather inert. The studies resolved the morphology of

[†] University of Aarhus.
[‡] Haldor Topsøe A/S.

(1) Topsøe, H.; Clausen, B. S.; Massoth, F. E. *Hydrotreating Catalysis*; Catalysis−Science and Technology, Vol. 11; Springer-Verlag: Berlin-Heidelberg, 1996.
(2) Prins, R.; de Beer, V. H. J.; Somorjai, G. A. *Catal. Rev.-Sci. Eng.* **1989**, *31*, 1−41.
(3) Prins, R. *Adv. Catal.* **2002**, *46*, 399−464.
(4) Whitehurst, D. D.; Isoda, T.; Mochida, I. *Adv. Catal.* **1998**, *42*, 345−471.
(5) Knudsen, K. G.; Cooper, B. H.; Topsøe, H. *Appl. Catal. A* **1999**, *189*, 205−215.
(6) Song, C. *Catal. Today* **2003**, *86* (1−4), 211−263.
(7) Hayden, T. F.; Dumesic, J. A. *J. Catal.* **1987**, *103*, 366−384.
(8) Shido, T.; Prins, R. *J. Phys. Chem. B* **1998**, *102*, 8426−8435.
(9) Kooyman, P. J.; Hensen, E. J. M.; de Jong, A. M.; Niemantsverdriet, J. W.; van Veen, J. A. R. *Catal. Lett.* **2001**, *74*, 49−53.
(10) de Jong, A. M.; de Beer, V. H. J.; van Veen, J. A. R.; Niemantsverdriet, J. W. *J. Vac. Sci. Technol. A* **1997**, *15*, 1592−1596.
(11) Helveg, S.; Lauritsen, J. V.; Lægsgaard, E.; Stensgaard, I.; Nørskov, J. K.; Clausen, B. S.; Topsøe, H.; Besenbacher, F. *Phys. Rev. Lett.* **2000**, *84*, 951−954.
(12) Lauritsen, J. V.; Helveg, S.; Lægsgaard, E.; Stensgaard, I.; Clausen, B. S.; Topsøe, H.; Besenbacher, F. *J. Catal.* **2001**, *197*, 1−5.
(13) Lauritsen, J. V.; Bollinger, M. V.; Lægsgaard, E.; Jacobsen, K. W.; Nørskov, J. K.; Clausen, B. S.; Topsøe, H.; Besenbacher, F. *J. Catal.* **2004**, *221*, 510−522.

10.1021/ja0651106 CCC: $33.50 **© 2006 American Chemical Society**

individual single-layer MoS_2 nanoclusters in detail and allowed the first direct mapping of the MoS_2 edge sites responsible for the hydrodesulfurization (HDS) activity.[11] These studies confirmed that sulfur vacancies, which are assumed to be the reactive sites for the extrusion of sulfur in the HDS process, preferentially form at the edge of MoS_2 layers and not on the inactive (0001) basal plane of the MoS_2 nanoclusters. Furthermore, the STM studies revealed the existence of an interesting type of active sites associated with one-dimensional, metallic edge states at the brim of the MoS_2 nanoclusters.[14,15] The metallic brim sites were subsequently shown to be preferential adsorption sites for S-containing molecules (such as thiophene), which can facilitate hydrogenation and partial hydrogenolysis of the sulfur-containing molecules in the presence of hydrogen.[14,15] Theoretical studies concluded that the gold substrate did not perturb the metallic edge states significantly, and the model system consisting of gold-supported MoS_2 nanoclusters is therefore considered to reflect MoS_2 with a very weak cluster−support interaction strength. However, the strength and nature of the support interactions are parameters known to be important for the reactivity of MoS_2 in the real catalyst, and we therefore investigate the morphology and atomic-scale structure of MoS_2 nanoclusters synthesized on a graphite surface to study the effect of a more realistic model support.

The most widely used support for the MoS_2-based hydrotreating catalysts is γ-alumina, since the porous structure and the bonding properties of this metal oxide favor the synthesis of small MoS_2 clusters with a high edge dispersion, a high promoter loading, and consequently a high reactivity. However, the exact nature of the bonding of the active MoS_2 nanoclusters to the support and its influence on the activity is still a matter of extensive debate. In the literature, an increased activity has been correlated with the existence of so-called type II CoMoS structures,[1,16] which are assumed to be cobalt-promoted MoS_2-like clusters having a weak support interaction, as opposed to the less-active type I CoMoS structures that interact strongly with the support.[17−19] The lower activity of the type I phase is normally attributed to the formation of strong Mo−O−Al linkages to the support, which modifies the coordination and bonding of the reactive edge sites at the cluster edges. It was recently shown by Hinnemann et al.[20] in a theoretical study that both the electronic edge structure and the sulfur bonding strength (i.e., the tendency to form sulfur vacancies) were much influenced by the presence of oxygen linkages to the support, thus supporting this explanation. The more active type II structures typically form at higher sulfiding temperatures[16] by breaking the Mo−O−Al linkages, but the higher temperatures also lower the degree of edge dispersion due to sintering and lead to a loss of activity. Different methods have been developed to prevent this problem, including the use of chelating agents,[21] but also the choice of substrate can be used as a means of optimizing the formation of type II structures. In this regard, graphite as a substrate is indeed very interesting since carbon-supported MoS_2-based hydrotreating catalysts are found to exhibit a very high HDS reactivity.[22−25] For these reasons we have undertaken a study of the nature of the bonding of MoS_2 to a graphite model substrate. In previous studies, the level of graphitization seems to vary for the carbon support, and therefore we also study the support effect on defective graphite surfaces. The atom-resolved STM images provide information on the atomic-scale structure and morphology of MoS_2 nanoclusters supported on graphite, and it is shown that STM is sensitive to the MoS_2/graphite interface, thus allowing the first detailed investigation of the bonding of MoS_2 to graphite.

2. Experimental Section

The experiments are performed in an ultrahigh-vacuum (UHV) chamber with a base pressure below 1×10^{-10} mbar. The chamber is equipped with standard equipment for surface preparation and analysis and a home-built high-resolution scanning tunneling microscope. A graphite sample [highly oriented pyrolytic graphite (HOPG), Structure Probe, Inc., grade SPI-2] was used as a support for the growth of MoS_2 nanoclusters. Prior to the experiments, the HOPG crystal, used as a substrate for the synthesis of MoS_2 nanoclusters, was cleaved in air with adhesive tape to expose the atomically flat (0001) basal plane. After transfer to the UHV chamber, the sample was thoroughly degassed at 1200 K to provide a clean and adsorbate-free substrate. When the substrate was imaged at this stage, STM revealed clean and atomically flat terraces extending typically over several hundred nanometers. For the synthesis of MoS_2 supported on the graphite surface, metallic molybdenum (99.9% nominal purity) was evaporated onto the substrate using an e-beam evaporator (Oxford Applied Research, EGCO-4). The deposition rate was calibrated prior to the synthesis to $\sim 1.7 \times 10^{-4}$ monolayer/s by monitoring, in high-resolution STM images, the coverage of Mo on a Au(111) surface, which forms a well-characterized reference.[11] The chemical purity of the deposited Mo was checked with Auger electron spectroscopy. For the subsequent sulfidation, gaseous hydrogen sulfide (H_2S) was dosed to the vacuum system from a lecture bottle (99.8% nominal purity), with hydrogen accounting for the major part of the 0.2% impurities, as confirmed by rest gas analysis during synthesis.

2.1. Synthesis of the Model System: MoS_2 Nanoclusters on HOPG(0001). An atomically resolved STM image of the clean HOPG surface is shown in Figure 1a. The graphite(0001) surface exposes a honeycomb structure consisting of sp^2-hybridized carbon atoms, which occupy nonequivalent sites within the two-dimensional surface unit cell: α carbon atoms, which have neighbors in the underlying layer, and β carbon atoms, which have none, as shown in the ball model in Figure 2. It has previously been shown in detail that constant-current STM resolves only the β-sites of the graphite surface.[26−28] This is due to the fact that STM images in general reflect a convolution of the geometric and the electronic structures of the surface.[29,30] It is thus not

(14) Lauritsen, J. V.; Nyberg, M.; Vang, R. T.; Bollinger, M. V.; Clausen, B. S.; Topsøe, H.; Jacobsen, K. W.; Lægsgaard, E.; Nørskov, J. K.; Besenbacher, F. *Nanotechnology* **2003**, *14*, 385−389.
(15) Lauritsen, J. V.; Nyberg, M.; Nørskov, J. K.; Clausen, B. S.; Topsøe, H.; Lægsgaard, E.; Besenbacher, F. *J. Catal.* **2004**, *224*, 94−106.
(16) Candia, R.; Clausen, B. S.; Bartholdy, J.; Topsøe, N.-Y.; Lengeler, B.; Topsøe, H. *Proceedings of the 8th International Congress on Catalysis*; Verlag Chemie: Weinheim, 1984; Vol. II, page 375.
(17) Topsøe, H.; Clausen, B. S. *Appl. Catal.* **1986**, *25*, 273−293.
(18) van Veen, J. A. R.; Gerkema, E.; van der Kraan, A. M.; Hendriks, P. A. J. M.; Beens, H. *J. Catal.* **1992**, *133*, 112−123.
(19) Hensen, E. J. M.; de Beer, V. H. J.; van Veen, J. A. R.; van Santen, R. A. *Catal. Lett.* **2002**, *84*, 59−67.
(20) Hinnemann, B.; Nørskov, J. K.; Topsøe, H. *J. Phys. Chem. B* **2005**, *109*, 2245.
(21) Medici, L.; Prins, R. *J. Catal.* **1996**, *163*, 38−49.
(22) Breysse, M.; Bennett, B. A.; Chadwick, D.; Vrinat, M. *Bull. Soc. Chim. Belges* **1981**, *90*, 1271−1277.
(23) Duchet, J. C.; van Oers, E. M.; de Beer, V. H. J.; Prins, R. *J. Catal.* **1983**, *80*, 386-402.
(24) Topsøe, H.; Clausen, B. S. *Catal. Rev.-Sci. Eng.* **1984**, *26*, 395−420.
(25) Vissers, J. P. R.; Scheffer, B.; Debeer, V. H. J.; Moulijn, J. A.; Prins, R. *J. Catal.* **1987**, *105*, 277−284.
(26) Batra, I. P.; Garcia, N.; Rohrer, H.; Salemink, H.; Stoll, E.; Ciraci, S. *Surf. Sci.* **1987**, *181*, 126−138.
(27) Tomanek, D.; Louie, S. G.; Mamin, H. J.; Abraham, D. W.; Thomson, R. E.; Ganz, E.; Clarke, J. *Phys. Rev. B* **1987**, *35*, 7790−7793.
(28) Hembacher, S.; Giessibl, F. J.; Mannhart, J.; Quate, C. F. *Proc. Natl. Acad. Sci. U.S.A.* **2003**, *100*, 12539−12542.
(29) Tersoff, J.; Hamann, D. R. *Phys. Rev. B* **1985**, *31*, 805−813.

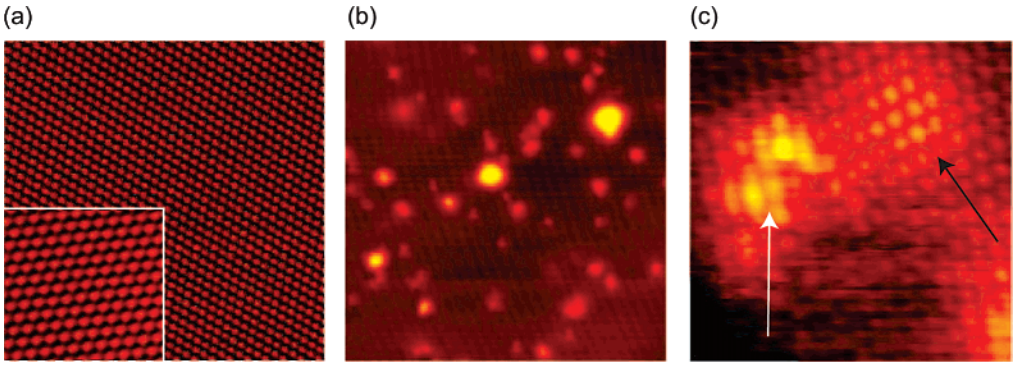

Figure 1. (a) STM image (80 Å × 80 Å, $I_t = 0.44$ nA and $V_t = -9.8$ mV) of the β-site atoms in the clean and flat HOPG surface. The inset shows a close-up (30 Å × 30 Å, $I_t = 0.24$ nA and $V_t = -7.9$ mV). (b) STM image (400 Å × 400 Å) of a defect-covered HOPG surface after the Ar^+ ion sputtering. (c) STM image (35 Å × 35 Å, $I_t = 0.44$ nA and $V_t = -9.8$ mV) of two types of defects on the HOPG surface.

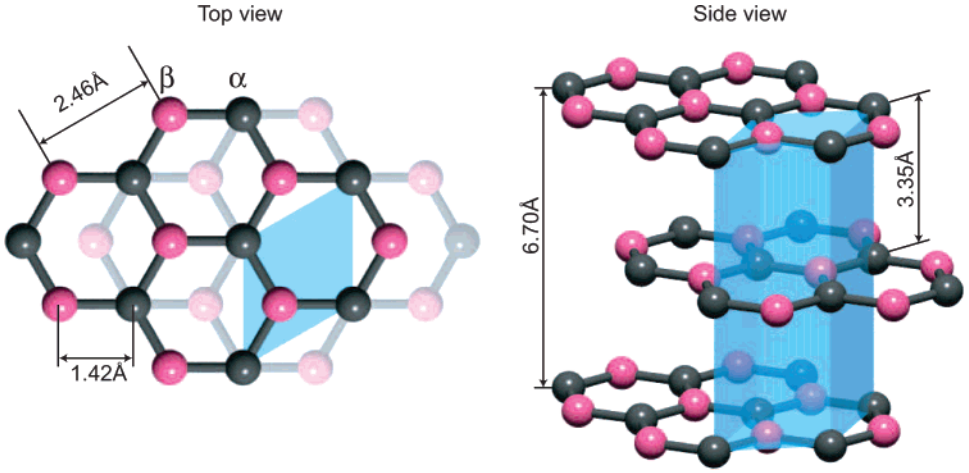

Figure 2. Ball model (top and side views, respectively) of the HOPG(0001) surface with two different carbon atoms, α and β sites. Only the β sites are visible in the STM images. The parallelepiped shows the unit cell.

valid in general to assume that maxima of the surface topography coincide with maxima observed in STM images, and this effect becomes especially important for band gap materials like MoS_2, or surfaces with directional bonding like graphite. The β-atoms of the graphite surface are indeed associated with a higher local density of states (LDOS) at the Fermi level compared to the α-atoms, and consequently the β-sites are imaged as protrusions by the STM, although they do not physically protrude from the surface. The distance between protrusions is measured to be 2.46 Å in STM images like Figure 1a, which is in accordance with the interatomic distance between the β-sites.

Images of metallic Mo evaporated onto HOPG revealed that the nucleation density of Mo on pristine HOPG was quite low, and Mo has a tendency to agglomerate at the step edges at the synthesis temperatures. It was not possible to synthesize highly dispersed MoS_2 nanoclusters on the as-cleaved HOPG, and we attribute this to a weak bonding to the (0001) graphite planes. Instead, we introduced a procedure involving a slight ion bombardment of the graphite prior to the Mo deposition, which resulted in a well-dispersed system. Figure 1b shows a large-scale STM image of the HOPG surface after ion bombardment with low-energetic Ar^+ ions (20 s at 150 eV acceleration voltage), followed by a flash annealing to 900 K. The ion bombardment is observed to introduce a low density of defects on the HOPG surface ($\sim 4 \times 10^{-4} - 10 \times 10^{-4}$ defects/Å^2).

The defects can be divided into two distinctive types, as depicted in Figure 1c. One type (black arrow) has as an almost circular dome-like structure showing the undisturbed lateral atomic arrangement of the (0001) HOPG surface, while the other (white arrow) exhibits a distorted atomic structure. The dome-like defects are attributed to interstitial atoms, either Ar or C.[31−33] This type of defect is not observed very often after the annealing to 900 K due to the desorption/mobility of the interstitials.[33] To a large degree, the much more abundant distorted type of defect appears unaffected by the annealing. The origin of this type of defect is associated with a distortion of the lattice atoms due to the formation of vacancies, since the Ar^+ ions are above the threshold (33.6 ± 1 eV) for creating vacancies.[34] The seemingly counterintuitive protruding imaging of defects associated with vacancies is explained by a vacancy-induced enhancement of the LDOS.[33,35] These vacancy defects are typically also associated with a long-range electronic perturbation on the HOPG surface, leading to a $(\sqrt{3}\times\sqrt{3})R30°$ superstructure in the images, which is in good agreement with previous studies of superstructures on HOPG caused by defects in the topmost layer.[36−38]

For the synthesis of nanocrystalline MoS_2 clusters, Mo (~10% of a monolayer) was first deposited onto the defective HOPG substrate at 400 K by physical vapor deposition in a sulfiding H_2S atmosphere corresponding to 5×10^{-6} mbar. Subsequently, the sample was

(30) Besenbacher, F. *Rep. Prog. Phys.* **1996**, *59*, 1737−1802.
(31) Kang, H.; Park, K. H.; Kim, C.; Shim, B. S.; Kim, S.; Moon, D. W. *Nucl. Instrum. Methods Phys. Res. Sect. B* **1992**, *67*, 312−315.
(32) Marton, D.; Bu, H.; Boyd, K. J.; Todorov, S. S.; Albayati, A. H.; Rabalais, J. W. *Surf. Sci.* **1995**, *326*, L489−L493.
(33) Hahn, J. R.; Kang, H. *Phys. Rev. B* **1999**, *60*, 6007−6017.
(34) Marton, D.; Boyd, K. J.; Lytle, T.; Rabalais, J. W. *Phys. Rev. B* **1993**, *48*, 6757−6766.
(35) Hahn, J. R.; Kang, H.; Song, S.; Jeon, I. C. *Phys. Rev. B* **1996**, *53*, R1725−R1728.
(36) An, B.; Fukuyama, S.; Yokogawa, K.; Yoshimura, M. *J. Appl. Phys.* **2002**, *92*, 2317−2322.
(37) Mizes, H. A.; Foster, J. S. *Science* **1989**, *244*, 559−562.
(38) Ruffieux, P.; Groning, O.; Schwaller, P.; Schlapbach, L.; Groning, P. *Phys. Rev. Lett.* **2000**, *84*, 4910−4913.

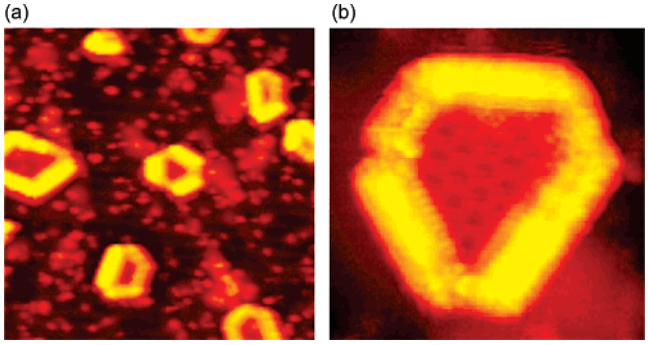

Figure 3. (a) STM image (430 Å × 430 Å, $I_t = 0.23$ nA and $V_t = -1250$ mV) of single-layer MoS_2 nanoclusters on HOPG. (b) STM image (150 Å × 150 Å, $I_t = 0.35$ nA and $V_t = -743$ mV) of a single-layer MoS_2 nanocluster.

annealed in a H_2S background pressure to facilitate full sulfidation and crystallization. The sample was then allowed to cool to 400 K in the H_2S atmosphere and transferred to the scanning tunneling microscope. This procedure is observed to result in crystalline MoS_2 nanoclusters dispersed on the terraces of the HOPG surface.

In accord with previous findings for the gold-supported systems[39] and other studies of high surface area catalysts,[40] it was found that the crystallinity, morphology, and stacking of the MoS_2 nanostructures were dependent on the subsequent annealing temperature. As will become clear in the following section, the clusters synthesized at 1000 K consist predominantly of a single S−Mo−S layer, whereas the clusters synthesized at 1200 K reflect multilayer clusters of typically 2−6 S−Mo−S layers. Clusters synthesized at lower temperatures, but at the same H_2S pressures used for the sulfidation step, showed a relatively poor crystalline order.

3. Results and Discussion

Figures 3a and 4a show large-scale STM images of the surface following the syntheses at 1000 and 1200 K, respectively. In both cases it is seen that the synthesis produces well-dispersed, nanocrystalline clusters on the HOPG surface. The atomically resolved STM images in Figure 3b and Figure 6a of the top facet of the nanoclusters synthesized at 1000 and 1200 K, respectively, reveal a crystalline MoS_2 basal plane consisting of hexagonally arranged protrusions with an average interatomic spacing of 3.15 Å. This observation agrees perfectly with the interatomic spacing of S atoms in the (0001) basal plane of MoS_2, and it is thus concluded that the clusters are MoS_2 nanoclusters aligned with the MoS_2(0001) face in parallel with the graphite substrate.

The most striking difference between clusters prepared at the two different postannealing temperatures is the apparent cluster height. In the most common 2H-MoS_2 stacking of molybdenite, the unit cell consists of two S−Mo−S layers separated by 6.15 Å, as shown in Figure 4. The basal plane of the MoS_2 clusters synthesized at 1000 K has an apparent height of 4.0 ± 0.3 Å relative to the HOPG measured from the basal plane of the cluster, and we therefore conclude that the clusters reflect *single-layer* MoS_2 nanoclusters (i.e., only one of the two building blocks of the unit cell is present in these clusters). The apparent height of the clusters synthesized at 1200 K is measured to be significantly higher than the expected interlayer distance. It is therefore concluded that the clusters prepared at 1200 K represent *multilayer* MoS_2 nanoclusters (i.e., consisting of two or more S−Mo−S layers). The height distribution of the synthesized clusters represents a measure of the stacking. It is found that the height of the predominant part of the clusters has values that fall in the range of ∼18−36 Å. When this is compared to the nominal step height of MoS_2(0001) of 6.15 Å, it is concluded that these values reflect cluster stacking of 2−5 layers and in rare cases even up to 6 S−Mo−S layers. As expected, the cluster coverage at 1200 K is lower than the coverage of clusters synthesized at 1000 K due to the stacking since the total amount of Mo was kept fixed. Taking the height into consideration, the total MoS_2 coverage is, for both systems, found to be ∼12−16% of a monolayer on average.

It is clearly observed in the STM images in Figures 3a and 4a that both the single-layer and the multilayer clusters preferentially adopt a hexagonal morphology. The exact shape of a MoS_2 nanocluster is determined in a simple model by the relative edge free energies of two different low-index edge terminations of the MoS_2(0001) basal plane, the $(10\bar{1}0)$ Mo-edge and the $(\bar{1}010)$ S-edge, respectively. Under equilibrium conditions, a single-layer cluster will prefer to expose a larger fraction of the more stable edge, and if the relative stability of one edge exceeds a factor of 2, a triangular shape will be the result, as was the case for our previous studies of single-layer MoS_2 nanoclusters on a Au(111) substrate. On the other hand, comparable stability of the two edge terminations will result in hexagonally truncated shape, as observed in the experiments (Figures 3a and 4a), and in the limit where the two edges are equally stable, the shape of the nanoclusters will be perfectly hexagonal. In the 2H-MoS_2 unit cell, the two S−Mo−S layers are translated and rotated 60° about the *c* axis, so that S atoms in one layer are placed on top of Mo atoms in the next layer. The edges of a multilayer cluster will thus expose both the Mo- and S-edge termination in an alternate fashion (see Figure 4c) and thus tend to cancel out any difference in edge free energies. Multilayer MoS_2 nanoclusters are consequently expected to form with hexagonal shapes. This observation is in good agreement with the STM observations of multilayer nanoclusters as depicted in Figure 4b.

It is, however, more surprising that the single-layer clusters display a hexagonally truncated shape, as opposed to the triangular shape found for the single-layer MoS_2 nanoclusters on a Au(111) substrate.[11] This change may, however, be explained by a change in synthesis parameters. The shape of MoS_2 clusters is known both experimentally[12,13] and theoretically[41,42] to be influenced by different synthesis parameters, such as the chemical potential of both hydrogen and sulfur (pressure, temperature) and the presence of promoter atoms. The increase in postannealing temperature in the present experiments from 673 to 1000 K, compared to the synthesis on Au(111),[11] was necessary to achieve full crystallinity of the clusters at the applied H_2S pressures. The increase in temperature leads to a lower chemical potential of sulfur, which may change the relative stability of the two types of edges, shifting the equilibrium shape from triangular, exposing only $(10\bar{1}0)$ Mo-edges, toward hexagonally truncated, exposing both types of edges.[41] A similar effect is observed when a mixture of H_2S

(39) Lauritsen, J. V. Atomic-scale study of a hydrodesulfurization model catalyst. Ph.D. Thesis, University of Aarhus, 2002.
(40) Chianelli, R. R.; Prestbridge, E. B.; Pecoraro, T. A.; DeNeufville, J. P. *Science* **1979**, *203*, 1105−1107.
(41) Schweiger, H.; Raybaud, P.; Kresse, G.; Toulhoat, H. *J. Catal.* **2002**, *207*, 76−87.
(42) Schweiger, H.; Raybaud, P.; Toulhoat, H. *J. Catal.* **2002**, *212*, 33−38.

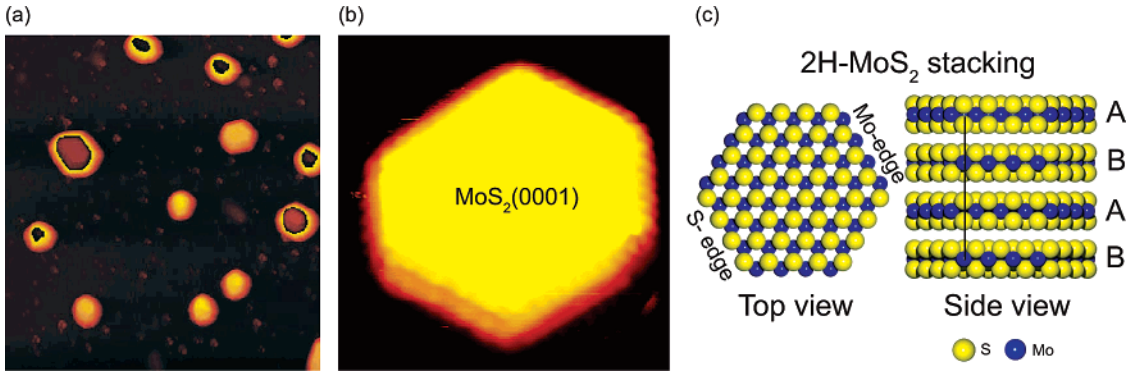

Figure 4. (a) STM image (1000 Å × 1000 Å, $I_t = 0.19$ nA and $V_t = -1250$ mV) of multilayer MoS_2 nanoclusters on HOPG synthesized at 1200 K. (b) STM image (69 Å × 70 Å, $I_t = 0.15$ nA and $V_t = -8.2$ mV) of a multilayer MoS_2 nanocluster. (c) Left: Ball model (top view) of a bulk truncated MoS_2 hexagon with Mo- and S-edges being exposed. Right: Ball model of the bulk 2H−MoS_2 stacking, where alternating layers exposes Mo- and S-edges successively.

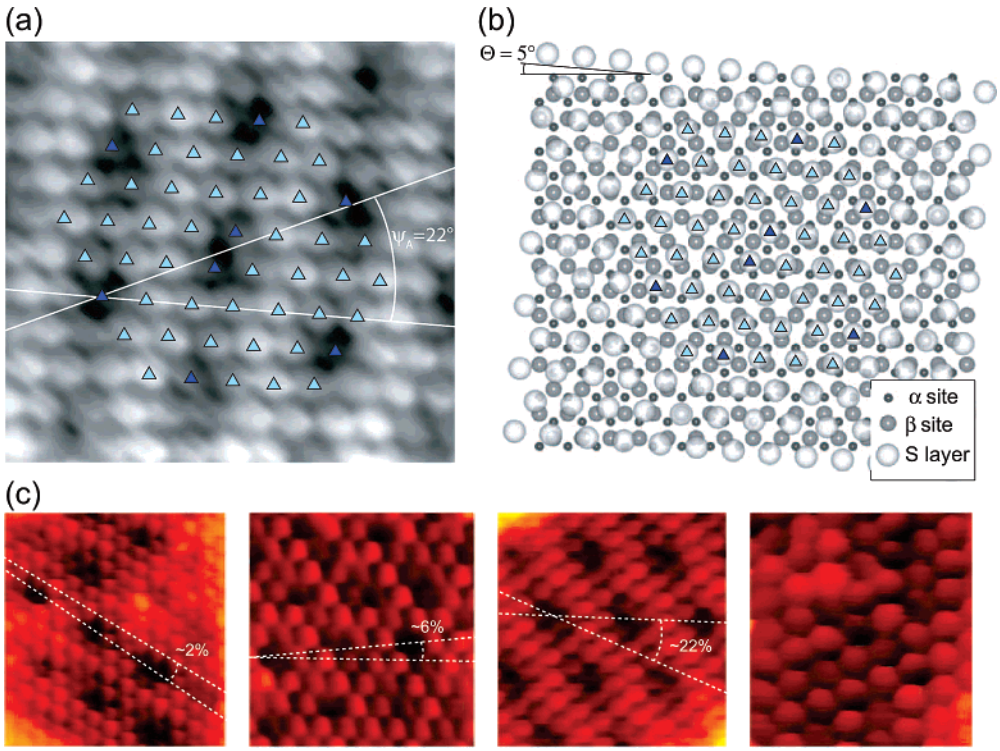

Figure 5. (a) STM image (35 Å × 33 Å, $I_t = 0.24$ nA and $V_t = -1250$ mV) showing the moiré superstructure on the basal plane of a single-layer MoS_2 nanocluster. (b) Ball model showing the HOPG lattice and a MoS_2 lattice rotated 5° with respect to each other. The triangles show that the resulting superimposed cluster/HOPG lattice structure explains the observed structure in the STM image nicely, with the dark regions (dark triangles) directly over the voids in the HOPG lattice. (c) STM images showing different moiré superstructures on the basal plane of single-layer MoS_2 nanoclusters. The rotation angles between the moiré structure and the MoS_2 lattice are approximately, from the left, 2, 6, and 22 Å, respectively. In the last image, no clear moiré pattern is observed.

and H_2 is used for the synthesis.[13] Furthermore, hydrogen adsorbs quite strongly on the fully sulfided S-edge and stabilizes the S-edge compared to the Mo-edge.[13,43−45] Hydrogen is always present during the synthesis in this experiment due to decomposition of H_2S in the vacuum system and gas inlet, and to the fact that commercially available H_2S gas with the highest nominal purity always contains about 0.2% hydrogen. It is therefore plausible that S-edges on single-layer MoS_2 synthesized on HOPG, apart from a stabilizing effect of the increased temperature, furthermore experience an additional stabilization of hydrogen, which makes the stability of the S-edges comparable to that of the Mo-edges, resulting in a hexagonally truncated cluster shape, as observed in the experiment.

3.1. Single-Layer MoS_2 on Graphite. In atom-resolved STM images of the single-layer MoS_2 clusters, a moiré superstructure is clearly observed to be superimposed on the hexagonal lattice of sulfur atoms on the basal plane (see Figure 5a). The moiré pattern arises from rotation and lattice mismatch between MoS_2 and HOPG. This pattern thus reveals information on the structure of the MoS_2−graphite interface. According to the principle of epitaxial rotation, the relationship between the rotation angle of the moiré structure relative to the MoS_2 lattice, ψ_A, and the

(43) Raybaud, P.; Hafner, J.; Kresse, G.; Kasztelan, S.; Toulhoat, H. *J. Catal.* **2000**, *189*, 129−146.
(44) Bollinger, M. V.; Jacobsen, K. W.; Nørskov, J. K. *Phys. Rev. B* **2003**, *67*, 085410.
(45) Cristol, S.; Paul, J. F.; Payen, E.; Bougeard, D.; Clémendot, S.; Hutschka, F. *J. Phys. Chem. B* **2002**, *106*, 5659−5667.

angle between the MoS_2 and substrate lattice, θ, is given as[46]

$$\cos\theta = r_{SA}\sin^2\psi_A + \cos\psi_A\sqrt{1 - r_{SA}{}^2\sin^2\psi_A} \quad (1)$$

where r_{SA} is the ratio of the substrate and MoS_2 lattice parameter. For the specific cluster in Figure 5a, the angle θ is found to be $22 \pm 1°$, which gives θ a value of 5° if the lattice parameter for HOPG is taken to be the distance between voids of the honeycomb structure on the HOPG surface. The angle between the MoS_2 lattice and the voids in the HOPG could also be measured directly in images with atomic resolution on both the MoS_2 and the HOPG and was found to be $5 \pm 1°$ for this particular cluster, in good agreement with the above.

We observe, however, a number of different periodicities of the moiré patterns on other clusters, as shown in Figure 5c, indicating that the rotation θ of the MoS_2 relative to the HOPG varies from cluster to cluster. This rotation is also directly observed when comparing the relative orientation of MoS_2 clusters located on the same HOPG terrace in large-scale images (e.g., Figure 3a). The variation of the rotation of the clusters indicates that the interaction between the MoS_2 basal plane and the HOPG lattice is indeed rather weak, since a stronger bonding presumably would favor a particular orientation.

The vertical corrugation in the moiré superstructures is measured in STM linescans to be 0.7−2 Å over the lateral distance of the specific moiré pattern (typically 9−12 Å). It is well known that MoS_2 is indeed very flexible perpendicular to the basal plane, which is exemplified by the formation of nanotubes and rag-like MoS_2 structures.[40,47−49] The magnitude of the corrugation in, e.g., Figure 5a is, however, unlikely to reflect only a geometrical relaxation of the 2.39 Å Mo−S bonds in MoS_2 over such short distances. The moiré pattern is therefore also considered to be related to an electronic effect of the MoS_2 adlayer on HOPG, which is also commonly observed on other transition metal−dichalgonide surfaces.[50]

A moiré pattern dominated by electronic effects is also consistent with the fact that the voids in the honeycomb structure of HOPG, which are associated with a low tunnel probability, seem to decide the structure of the moiré pattern rather than the geometrical structure of both types of carbon sites. The ball model in Figure 5b for the specific cluster in Figure 5a shows the HOPG lattice and a hexagonal lattice with an interatomic spacing of 3.15 Å, corresponding to the interatomic distance in MoS_2, where the latter is rotated 5° compared to the HOPG lattice. As seen from the triangles, the resulting superimposed cluster/HOPG lattice structure explains the structure observed in the STM images very well, if the dark regions (dark triangles) are positioned directly over the voids in the HOPG lattice.

The necessity of introducing defects in the surface region to stabilize a high dispersion of MoS_2 on the plane HOPG(0001) surface clearly shows that defects play an important role in the bonding of MoS_2 to graphite at elevated temperatures. The atom-resolved STM images provide information on the nature of the anchoring of the MoS_2 nanoclusters to the defects.

In the atom-resolved images, the interior basal planes of the single-layer MoS_2 nanoclusters mostly appear with a perfect crystalline order with the moiré pattern superimposed. Since the moiré pattern is very sensitive to the MoS_2−HOPG interface, the undistorted appearance also reflects that the topmost layer of graphite underneath is also perfectly crystalline. Occasionally, we do observe a distortion in the MoS_2 lattice on the basal plane of the clusters, but a simple comparison of the defect density and the average area of each cluster shows that the number of defects located underneath the MoS_2 basal plane is lower (0−2 defects per cluster) than the expected average number of 5−8 defects per cluster. It is therefore concluded that no substantial bonding of basal plane sites underneath the MoS_2 clusters to sites associated with defects in the graphite surface occurs.

In contrast, the appearance of the edges of the single-layer MoS_2 clusters indicates that defects are present in this region. The edges appear much brighter in the atom-resolved STM images, indicating that the LDOS is higher here, but the crystalline ordering is clearly perturbed in several regions at the edges. Both the size and interspacing between the perturbed edge regions suggest that defects are present in the graphite support directly under the edges. The observations suggest that the bonding of the cluster to the substrate forms predominantly through the edge sites of the MoS_2 nanocluster. This conclusion is also consistent with the notion that edge sites typically have a higher interaction strength than the rather inert basal planes of MoS_2.[1]

The observation that defects control the anchoring of the MoS_2 was investigated further by controlling the cluster size. In separate experiments, the duration of the 1000 K postannealing step was increased from 15 min to a total of 60 min, which led to the formation of ~3 times larger single-layer MoS_2 nanoclusters. Again, none of the larger clusters show a significant concentration of defects under the MoS_2 basal plane despite the larger size, confirming the observation above. Although the longer annealing time principally should favor the formation of a more homogeneous ensemble of clusters, the result was a much more complex morphology than the one shown in Figure 3a, now consisting of irregularly shaped single-layer clusters and clusters partly merged from the simpler shapes. The irregular cluster shapes cannot be explained by the simple Wulff-type arguments for a free MoS_2 cluster, but are rather attributed to defects controlling the morphology during growth. Presumably, the defects act as pinning sites during growth, and their distribution thus forces the clusters to adopt irregular shapes that deviate from the expectation of an unsupported cluster in thermodynamic equilibrium. Thus, two different driving forces seem to control the morphology during growth, namely the minimization of edge free energy of the clusters and the position of the adhesion points during growth.

3.2. Atomic-Scale Structure of Multilayer MoS_2 Edges. At the synthesis temperature of 1200 K, all MoS_2 nanoclusters appear as multilayer clusters. The absence of single-layer clusters is explained by a preferential three-dimensional growth of stacked MoS_2 nanoclusters at 1200 K. Although the sputter-induced defects remain on the HOPG substrate after preparation at 1200 K, it is clearly not favorable enough to support two-dimensional growth of single-layer MoS_2 nanostructures. This finding reflects that the adhesion of the topmost layers of the MoS_2 nanoclusters on lower layers is larger than that on the

(46) Grey, F.; Bohr, J. *Europhys. Lett.* **1992**, *18*, 717−722.
(47) Feldman, Y.; Wasserman, E.; Srolovitz, D. J.; Tenne, R. *Science* **1995**, *267*, 222−225.
(48) Seifert, G.; Terrones, H.; Terrones, M.; Jungnickel, G.; Frauenheim, T. *Phys. Rev. Lett.* **2000**, *85*, 146−149.
(49) Remskar, M. *Adv. Mater.* **2004**, *16*, 1497−1504.
(50) Kobayashi, K.; Yamauchi, J. *Phys. Rev. B* **1995**, *51*, 17085−17095.

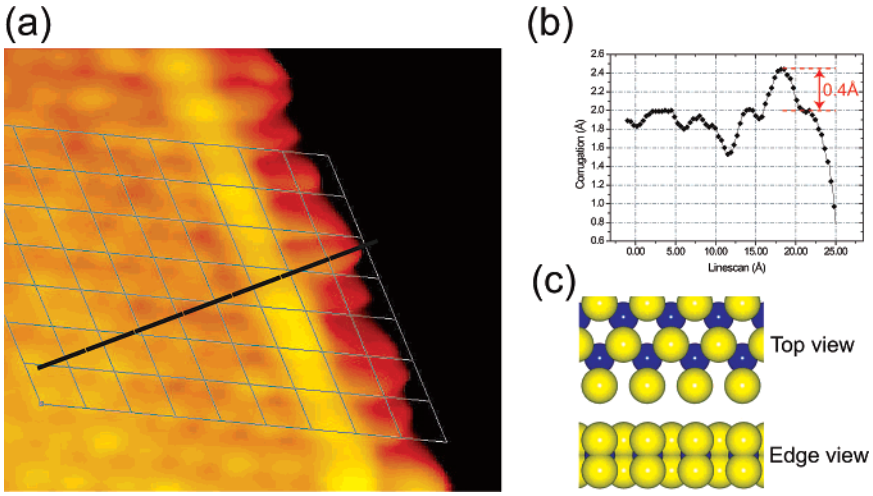

Figure 6. Atom-resolved STM image (36 Å × 35 Å, I_t = 0.23 nA and V_t = −7.9 mV) showing the atomic-scale structure of the (10$\bar{1}$0) Mo-edge on multilayer MoS_2 nanoclusters supported on HOPG. The superimposed grid on the basal plane sulfur atoms shows that protrusions at the edge are out of registry. (b) A linescan across the brim region of the Mo-edge. (c) A ball model (top and side view, respectively) of the Mo-edge fully saturated with sulfur dimers corresponding to the experiment (Mo, blue; S, yellow).

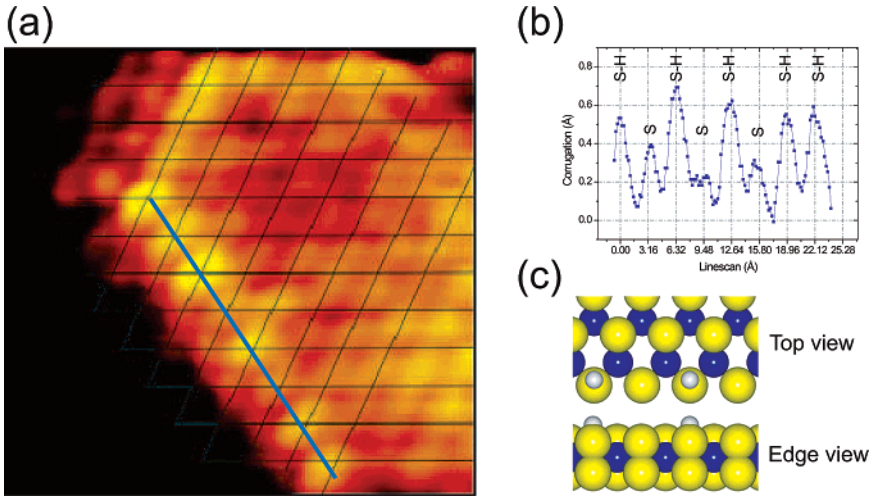

Figure 7. (a) Atom-resolved STM image (41 Å × 37 Å, I_t = 0.19 nA and V_t = 0.6 mV) of the ($\bar{1}$010) S-edge. The grid shows that protrusions on the S-edge are imaged in registry. (b) A linescan along the bright brim on the S-edge. Regions with lower intensity are associated with missing S−H groups. (c) A ball model of the fully sulfided S-edge and with a fractional coverage of S−H groups representing the experimental image of the S-edge (Mo, blue; S, yellow; H, gray).

graphite(0001) plane or on defects on the substrate. It is unlikely that the ordinary interlayer van der Waals bonding of the MoS_2 nanocluster basal planes is responsible for the preferential stacking. Instead, it is more likely that the stacking of the multilayer MoS_2 nanoclusters is facilitated by interlayer bonding at sites near the cluster perimenter due to the presence of electronic edge states localized at the two outermost atomic rows, which were previously shown to facilitate a strong bonding compared to basal plane sites.[14] The complete absence of stacked structures at lower temperature is then explained by a lower mobility of the surface species.

In atom-resolved STM images (Figures 6 and 7), the edge structure of the multilayer MoS_2 nanoclusters is resolved, and since the edge structure does not appear to be perturbed by the HOPG defects several layers underneath, their structure can be analyzed in detail. As expected from the hexagonal morphology of the multilayer clusters, two different types of edges aligned with a 120° angle between them are found in the atom-resolved images, implying that one is a (10$\bar{1}$0) Mo-type edge, whereas the other is a ($\bar{1}$010) S-edge. Figure 6a shows a close-up of one of the edge types on a three-layer-high hexagonal MoS_2 nanocluster. This edge is characterized by two predominant features: (i) protrusions at the edge are observed to be shifted relative to the registry of the S atoms on the basal plane, and (ii) a narrow bright brim exists, aligned in the direction parallel to the cluster edge just behind the outermost row of edge protrusions (see Figure 6b). These two observations are very similar to the signatures which unambiguously identified the fully sulfided Mo-edge in atom-resolved STM images of single-layer clusters grown on a gold substrate.[13,51] The qualitative accordance with previous observations therefore suggests that the edge analyzed in Figure 6a reflects a fully sulfided Mo-edge on the multilayer, graphite-supported clusters (see ball model in Figure 6c). For the multilayer clusters, the height of the brim above the basal plane is measured to be ∼0.4 Å. It is appealing that the brim height of the clusters synthesized on gold was also found to be 0.4 Å, although one should be cautious

(51) Bollinger, M. V.; Lauritsen, J. V.; Jacobsen, K. W.; Nørskov, J. K.; Helveg, S.; Besenbacher, F. *Phys. Rev. Lett.* **2001**, *87*, 196803.

when making quantitative comparisons between the STM images of MoS_2 clusters synthesized on HOPG and gold.

The fact that the protrusions on the fully sulfided Mo-edges are imaged *out* of registry with the basal plane S atoms and the appearance of the narrow bright brim cannot be explained by a simple geometric model of the edges. Instead, the appearances of the edges reflect a convolution of electronic and geometric features of the MoS_2 edge. As already mentioned in the Introduction, it was recently shown by detailed DFT calculations[44,51] that the Mo-edges of a free (or gold-supported) MoS_2 slab are metallic as opposed to the interior of the MoS_2, which is characterized as a semiconductor. Both the shifting of edge protrusions out of registry and the pronounced bright brim of the Mo-edge with sulfur dimers in Figure 6a can be reproduced qualitatively and quantitatively in STM simulations[41,51] and is traced back to two metallic edge states of this particular edge termination of MoS_2. One of the edge states originates from the overlap of p_x orbitals between the S dimers terminating the Mo-edges, and its structure implies that the STM primarily images the interstitial region between the S dimer pairs as bright, as also observed in Figure 6a.

The second edge state, pertaining to the fully sulfided Mo-edge, is associated with a hybridization of the 3d Mo states and the 2p S states and has a quite complicated structure, extending in the first few rows counted from the edge and inward, and is primarily responsible for the bright brim on the clusters in the STM image. Thus, the Mo-edge appears in STM images in a very similar way to the gold-supported system of MoS_2, and it is concluded that the same structure with the same catalytic properties is present in the graphite-supported multilayer structures.

The symmetry of the crystal implies that the other edge must be of the $(\bar{1}010)$ S-edge type, which is shown in Figure 7a. The primary indicator for the S-edge in atom-resolved STM images of MoS_2 nanoclusters is again the location of the brim and the registry of the protrusions at the edge. On the S-edge, the outermost row of protrusions appears with a quite weak contrast, and a superimposed grid shows that the protrusions are placed *in* registry with the basal plane S atoms. The STM images clearly show the existence of a brim located adjacent to the outermost row of protrusions. This brim is more intense than that of the corresponding Mo-edge also shown in the top part of the image. In contrast to the brim of the Mo-edge, which shows no systematic corrugation along the brim, the position of individual protrusions along the brim region of the S-edge is clearly resolved, with the regular interatomic spacing of 3.15 Å of MoS_2. However, it is also apparent from the images that the protrusions in the brim region show a systematic variation in height. This is depicted more clearly in the scan line of Figure 7b, where the height of the individual protrusions is shown relative to the basal plane. Two types of brim protrusions are present, with a difference in height of 0.2 Å, measured from peak to peak.

S-edges formed under highly sulfiding conditions were not observed previously with STM, since only Mo-edges are exposed for triangular single-layer structures formed under sulfiding conditions on Au(111).[11] It should, however, be noted that the appearance of the S-edge in the graphite case is similar to the sulfur edges imaged for hexagonally truncated, single-layer MoS_2 nanoclusters synthesized in a mixture of hydrogen and hydrogen sulfide (sulfo-reductive conditions).[13] In that case, a brim imaged with a height of 0.5 Å above the basal plane was observed, together with edge protrusions placed in registry with the S atoms on the basal plane, and the edges with this signature were identified with a combination of DFT studies and STM as fully sulfided S-edges with hydrogen adsorbed to form S−H groups. For comparison, the brim protrusions in Figure 7a are 0.3 and 0.5 Å above the basal plane, respectively. The similarities suggest that the S-edges of the multilayer MoS_2 clusters also expose this kind of termination, despite the fact that they are synthesized under more sulfiding conditions. As mentioned before, hydrogen is always present during the synthesis and in the background gas of the vacuum, and furthermore, it is found in theoretical DFT studies that hydrogen adsorbs quite strongly on the fully sulfided S-edge.[13,43−45] It is therefore plausible that a fractional population of S−H groups forms even at the low hydrogen pressures present in this experiment. Hydrogen adsorption on the S-edge with a less than 100% coverage may also explain the observation of the different brim heights along the edge, since the bonding of H on the S adjacent to the brim will most likely change the characteristics of the electronic states associated with the brim, which in this case seems to lead to a lowering of the intensity at sites which have no H attached. This configuration is shown in the ball model of Figure 7c.

The observation of H adsorbates even at the very low hydrogen background pressures used in the present experiments on the S-edge MoS_2 is very interesting in terms of understanding the catalytic role of these edges. To facilitate the HDS reaction, both the adsorption of the reacting S-containing molecule and the dissociation of H_2 into more reactive, loosely bound atomic H species is required. In particular, the fractional occupation of hydrogen on the S-edge is interesting in this respect, since free sites thus are available for vacancy formation or direct adsorption of molecules in the brim region, which can react with the adjacent atomic H species.

4. Conclusions

In conclusion, scanning tunneling microscopy is applied to investigate the atomic-scale structure and morphology of single-layer and multilayer MoS_2 nanoclusters synthesized on a graphite substrate. These studies include for the first time the effects of a realistic support material in hydrotreating model studies.

The interaction between MoS_2 and the pristine HOPG(0001) surface is observed to be too weak to support a high dispersion of MoS_2 nanoclusters on the substrate. Instead, a HOPG substrate, pretreated by ion bombardment to create a low density of surface defects, was used. The synthesized MoS_2 nanoclusters are observed to display a very temperature-dependent morphology, since clusters prepared at 1000 K grow as single-layer clusters, whereas clusters prepared at 1200 K exclusively grow as stacked multilayer clusters.

For single-layer structures synthesized at 1000 K, the interface structure between the S−Mo−S layer and the HOPG is reflected in the atomic details of STM images, and we pinpoint the anchoring sites of the MoS_2 nanoclusters as surface defects preferentially located directly underneath the nanoclusters edges and not the basal plane. The preferential morphology of single-layer MoS_2 nanoclusters is observed to be hexagonal, indicating

that this is the equilibrium shape under the conditions of the experiment, but for larger clusters the morphology was observed to be significantly more complex due to pinning of the cluster edges to defects.

The multilayer clusters are predominantly shaped as hexagons and exhibit a stacking of typically 2 to 5 S−Mo−S layers. The catalytically important edges of the MoS_2 nanoclusters are characterized in terms of atom-resolved STM images of the top facet of the MoS_2 nanoclusters, and it is found that two types of low-index MoS_2 edges are present. One type is identified as the $(\bar{1}010)$ Mo-edge fully saturated with sulfur, whereas the other is characterized as the fully sulfided $(10\bar{1}0)$ S-edge with approximately 50% coverage of hydrogen.

Importantly, the atom-resolved STM images provide solid evidence for one-dimensional metallic brim sites on the graphite-supported MoS_2, which were previously shown to play an important role in the catalytic properties of single-layer MoS_2.[14,15] Finally, from a catalytic point of view, the observation of hydrogen adsorbates at the clusters edges is highly interesting, since both adsorption of the S-containing molecule and dissociation of H_2 are required to facilitate the HDS reaction.

In future experiments, it would be interesting to study the selective adsorption of S-containing probe molecules like thiophene (C_4H_4S). Such a study has previously been carried out for the Au-supported model system,[14] and similar atom-resolved STM studies of the model system described in this report might give new insight into the fundamental question of which type of low-index edge structure of MoS_2 is more active, or if both edges are involved in HDS reactions.

Acknowledgment. This work was supported by the Danish Ministry of Science, Technology, and Innovation through the iNANO center. J.V.L. acknowledges support from the Carlsberg Foundation.

JA0651106